EPiC Series in Computing

Volume 58, 2019, Pages 75–82

Proceedings of 34th International Conference on Computers and Their Applications

New classes of monohedral spherical tilings by non-convex spherical hexagons and non-convex spherical pentagons with GeoGebra

Ana Maria D'Azevedo Breda[1] and José Manuel Dos Santos Dos Santos[2]

[1] Universidade de Aveiro, Departamento de Matemática, Aveiro, Portugal
ambreda@ua.pt

[2] Universidade Aberta, Departamento de Ciências e Tecnologia, Lisboa, Portugal
dossantosdossantos@gmail.com

Abstract

In previous works we have ilustrate a procedure to obtain spherical tiling with GeoGebra. We have found new classes of monohedral spherical tiling by four spherical pentagons, and new class of dihedral spherical tiling by twelve spherical pentagons. One again, we would make use of GeoGebra to show how we can do generate new classes of monohedral non-convex hexagonal spherical tilings, $\mathfrak{H}_{(\mathscr{C},\tau)}$, changing the side gluing rules of the regular spherical octahedral tiling, by local action of particular subgroups of spherical isometries.

In relation to one of the new classes, by hexagonal tiles, we describe some of its properties. We also show the existence of a a new family of monohedral pentagonal tiling which arises as a degenarated case associated to the family $\mathfrak{H}_{(\mathscr{C},0)}$. All these classes of spherical tilings have emerged as a result of an interactive construction process, only possible by the use of newly produced GeoGebra tools and the dynamic interaction capabilities of this software.

1 Introduction

Spherical tilings by right triangles were obtained by Yukako Ueno and Yoshio Agaoka in 1996 [20]. Later, in 2002, the complete classification of monohedral edge-to-edge triangular spherical tilings was achieved by the same authors [21]. They have extended the classification of triangular f-spherical foldings, studied and characterised by Ana Breda, in 1992,[3].

The classification of spherical tilings by triangles is not yet completed. In fact, little is known when the condition of being monohedral or edge-to-edge is dropped out.

The combinatorial study of spherical tilings by twelve pentagons considering all vertices of valence greater than or equal to three has been also achieved, see [11] for details. Very little is known about spherical tilings involving non-convex spherical polygons, namely, tilings where the possibility of vertices of valence two should not be dismissed. Recently, a family of spherical monohedral tiles by four congruent and non-convex spherical pentagons has been characterised [6].

Besides the theoretical mathematical aspects involved in the study of spherical tilings, they are also object of interest in other areas of knowledge and in technological applications. Walter Kohn report that the year 1984 brought a big surprise in the field of crystallography. He refers the work of:

> "D. Schechtman and co-workers that reported a beautiful x-ray pattern with unequivocal icosahedral symmetry for rapidly quenched AlMn compounds. The appropriate theory was independently developed by D. Levine and P. Steinhardt, who coined the words quasicrystal and quasiperiodic. Even more curious was the fact that R. Penrose (1984) had anticipated these concepts in purely geometric [terms], so-called Penrose tilings" [13, p. s70].

Findings of this kind reinforce the need to continue studying geometric patterns and their properties. Spherical tiling has also applications to chemistry. For instance, in the study of periodic nanostructures [10], emerging new forms of association of molecules, notably fullerenes [9], leading to a deeper study of spherical tilings by triangles, squares, pentagons [17]. In the same line of reasoning other tilings including heptagons[19] and heptagons and octagons[18] had emerged. Applications to new possibilities for new molecular patterns are exposed in [22, 15, 16, 12, 7]. Nowadays, in engineering there is a need to merge the computer aided design and computer aided engineering into a single approach, contributing to an increasing interest in studying relationships between spherical tilings and spherical Bezier curves [8]. The knowledge of spherical tilings can also be useful for the developed of some issues in computational algebra [14]. The facility location problems, spherical designs and minimal energy point configurations on spheres [1, 2] are other fields where the study of spherical tilings is quite useful.

In this article we intend to extend the knowledge of the set of spherical tilings, here denoted by $\mathfrak{T}$, presenting and characterising subsets of hexagonal spherical tilings, as well as new patterns of pentagonal tilings.

2 Related Work

It is a well-known fact that it is not possible to find a monohedral tiling of the sphere by convex spherical hexagons whose vertices have valence equal to three. however, we are interested in study tilings of the sphere by non-convex spherical polygons, so we was interesting in study the existence of monohedral tiling by non-convex spherical hexagons, with some vertices with valence equal to two. In a tiling of the sphere by spherical polygons, at vertices of valence two are associated two angles whose sum is 2π, a situation that posed further problems to the investigation of the existence of such tilings. These situations may be solved making use of the dynamic capabilities of GeoGebra that have been proved to be interesting for our research.

We had create tools in GeoGebra to spherical geometry, initially we use these tools to obtain some well known spherical tilings and provide illustrations of some new spherical tilings [5]. Namely, we found a new family of tilings of the sphere, $\widehat{\mathfrak{B}_{\frac{p}{q}}}$, $p,q \in \mathbb{N}$, are presented. This family contains the well known antiprismatic tilings, wich is identified and obtained by a global action of a subgroup of spherical isometries , see [4] .

A proper adaptation to the procedure previously described to characterise the one-parameter family of tilings, $\mathfrak{P}_{(\mathscr{C},\tau)}$ with $\tau \in]0,\pi[\setminus\{\frac{1}{2}\arccos(-\frac{1}{3})\}$, by four congruent spherical non convex pentagons, see [6], determines one-parameter family of monohedral spherical hexagonal tiling with six faces, $\mathfrak{H}_{(\mathscr{C},\tau)}, \tau \in \left]0, \arcsin\left(\frac{\sqrt{6}}{3}\right) + \frac{\pi}{2}\right[\setminus \{\arctan\left(\frac{\sqrt{2}}{2}\right)\}$.

3 Methodology

Consider one of the triangular faces, $[A,B,C]$, of the regular octahedrical spherical tiling. Without loss of generality we may assume that the equilateral, spherical triangle $[ABC]$ of angles $\frac{\pi}{2}$, has as vertices the points A,B,C whose coordinates are respectively $(1,0,0),(0,1,0),(0,0,1)$. Let Q, S and R be the midpoints of the arcs $\widehat{AB}$, $\widehat{BC}$ and $\widehat{CA}$, respectively.

Having in mind, the use of a similar procedure as the one indicated in the end of the previous section, we study the tilings arising from the dynamic displacement of a point P, in the arc $\widehat{QC}$ making an angle of $\frac{\pi}{2}$ with the arc $\widehat{AB}$, and the spherical point $D=(\frac{\sqrt{3}}{3},-\frac{\sqrt{3}}{3},\frac{\sqrt{3}}{3})$, crucial to the definition of the set

$\mathscr{C}=\{X\in S^2 : X\in\widehat{PS}\vee X\in\widehat{PR}\vee X\in\widehat{PQ}\vee X\in\widehat{DR}\}$,

which is the starting cell for the generation of the tilings, see figure 1.

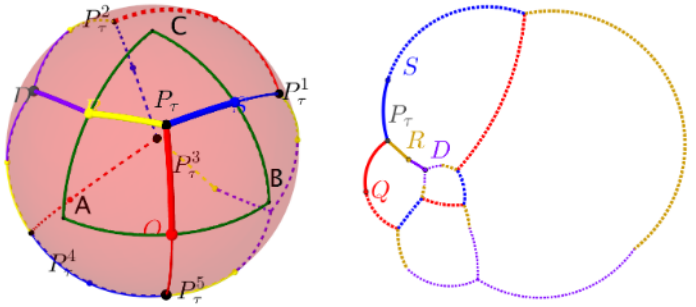

(a) $\mathfrak{H}_{(\mathscr{C},\frac{pi}{4})}$ (b) Cell $\mathscr{C}$ in the and planar graph.

Figure 1: Monohedral spherical tiling $\mathfrak{H}_{(\mathscr{C},\frac{\pi}{4})}$ and one of its planar graph.

It should be pointed out that without the dynamic properties of GeoGebra, the approach here described would not be possible. The number of simulations to be performed to have some insights about the behaviour of the created spherical patterns would be behind the imagination.

As we will see the use of GeoGebra for making explorations and the use of some of the symmetries of the octahedral tiling end up with the one parameter family of tilings $\mathfrak{H}_{(\mathscr{C},\tau)}$. The details will be given in the following section.

4 Experimental Results

The construction of the one parameter family of tilings $\mathfrak{H}_{(\mathscr{C},\tau)}$, $\tau\in\left]0,\arcsin\left(\frac{\sqrt{6}}{3}\right)+\frac{\pi}{2}\right[\setminus\{\arctan\left(\frac{\sqrt{2}}{2}\right)\}$ is based in the case where $P\in\widehat{QC}$ and $\widehat{QOP}=\tau$.

The points defining the cell $\mathscr{C}$ have respectively the coordinates:

$Q=(\cos(\frac{\pi}{4}),\sin(\frac{\pi}{4}),0)$;
$R=(\cos(\frac{\pi}{4}),0,\sin(\frac{\pi}{4}))$;
$S=(0,\cos(\frac{\pi}{4}),\sin(\frac{\pi}{4}))$;
$D=(\frac{\sqrt{3}}{3},-\frac{\sqrt{3}}{3},\frac{\sqrt{3}}{3})$;
$P=(\cos(\tau),0,\sin(\tau))$.

First we note that there is three cases where $\mathfrak{H}_{(\mathscr{C},\tau)}$ does not correspond to a hexagonal tiling. In fact, for $\tau = 0$ we have a monohedral tiling with six spherical pentagons (fig 2(a)). This spherical tiling belongs to a family of two parameters not yet studied. In fact it corresponds to a family of spherical tilings, by six non-convex spherical pentagons, defined starting from eleven vertex points: six of valence two; two of valence three; and four of valence four.

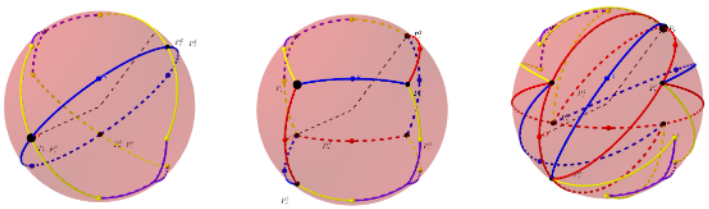

(a) $\mathfrak{H}_{(\mathscr{C},0)}$ (b) $\mathfrak{H}_{(\mathscr{C},\arctan\left(\frac{\sqrt{2}}{2}\right))}$ (c) $\mathfrak{H}_{(\mathscr{C},\arcsin\left(\frac{\sqrt{6}}{3}\right)+\frac{\pi}{2})}$

Figure 2: Degenerated cases of $\mathfrak{H}_{(\mathscr{C},\tau)}$.

If τ is equal to $\arctan\left(\frac{\sqrt{2}}{2}\right)$ we get a tiling by six congruents spherical "squares", this tiling correspond to the monohedral hexahedral tiling of the sphere (fig 2(b)). For τ equal to $\arcsin\left(\frac{\sqrt{6}}{3}\right)+\frac{\pi}{2}$, we end up with a dihedral spherical tiling composed by six congruent spherical pentagons and six congruent spherical digons (fig 2(c)).

For values of $\tau^* \in \left]0, \arcsin\left(\frac{\sqrt{6}}{3}\right)+\frac{\pi}{2}\right[\setminus \{\arctan(\frac{\sqrt{2}}{2})\}$ we have tilings of the sphere by six spherical non-convex hexagons, with fourteen vertices, six vertices with valence two and the other eighth vertices of valence three.

Looking at the illustration given in figure 1(a), the points P_τ^i are vertices of the tiling and the points Q and S are exactly the midpoints of two edges of the tiling. The arc measure of the elements of $\mathscr{C}$ are:

$\widehat{PQ} = \tau = c$

$\widehat{PR} = \widehat{PS} = \arccos\left(\frac{1}{2}\cos(\tau) + \frac{\sqrt{2}}{2}\sin(\tau)\right) = b$

$\widehat{DR} = \arccos\left(\frac{\sqrt{6}}{3}\right) = a.$

Each element of this family of tilings has one non-convex hexagonal prototile, with the following edge cyclic configurations $(a,b,2b,2c,b,a)$.

The angles defined by the arcs specified bellow are:

$$\widehat{SPQ} = \arccos\left(\frac{\frac{1}{2}-\cos x\left(\frac{\cos x}{2}+\frac{\sin x}{\sqrt{2}}\right)}{\sqrt{1-\cos^2(x^2)}\sqrt{1-\left(\frac{\cos x}{2}+\frac{\sin x}{\sqrt{2}}\right)^2}}\right)$$

$\widehat{SPQ} = \widehat{QPR}$

$\widehat{RPS} = 2\pi - 2\widehat{SPQ}$

$$\widehat{PRD} = \arccos\left(\frac{\sqrt{3}\left(\frac{\sin x}{\sqrt{3}}-\sqrt{\frac{2}{3}}\left(\frac{\cos x}{2}+\frac{\sin x}{\sqrt{2}}\right)\right)}{\sqrt{1-\left(\frac{\cos x}{2}+\frac{\sin x}{\sqrt{2}}\right)^2}}\right)$$

$\widehat{RDR_4} = \frac{2\pi}{3}$

For obtaining the spherical tilings, $\mathfrak{H}_{(\mathscr{C},\tau)}$, we consider the following set of spherical isometries, $\mathscr{I} = \{\mathscr{R}_{(S,\pi)}, \mathscr{R}_{(Q_1,\pi)}, \mathscr{R}_{(S_2,\pi)}, \mathscr{R}_{(Q_3,\pi)}, \mathscr{R}_{(S_3,\pi)}\}$ composed by five rotations, identified by its center and angle, where $Q_1 = \mathscr{R}_{(S,\pi)}(Q)$, $S_2 = \mathscr{R}_{(S,\pi)}(Q_1)$, $Q_3 = \mathscr{R}_{(S_2,\pi)}(Q_1)$, $S_3 = \mathscr{R}_{(S_2,\pi)}(Q_3)$.

The matricial representation of the element of $\mathscr{I}$ is given by:

$$\mathscr{R}_{(S,\pi)} = \mathscr{R}_{(Q_3,\pi)} = \begin{pmatrix} -1 & 0 & 0 \\ 0 & 0 & 1 \\ 0 & 1 & 0 \end{pmatrix}; \qquad \mathscr{R}_{(S_2,\pi)} = \begin{pmatrix} 0 & 1 & 0 \\ 1 & 0 & 0 \\ 0 & 0 & 1 \end{pmatrix};$$

$$\mathscr{R}_{(Q_1,\pi)} = \mathscr{R}_{(S_3,\pi)} = \begin{pmatrix} 0 & 0 & -1 \\ 0 & -1 & 0 \\ -1 & 0 & 0 \end{pmatrix}.$$

Consider $\mathscr{C}^0 = \mathscr{C}$ (graphically represented in figure 1(b)), $\mathscr{C}^1 = \mathscr{R}_{(S,\pi)}(\mathscr{C}^0)$, $\mathscr{C}^2 = \mathscr{R}_{(Q_1,\pi)}(\mathscr{C}^1)$, $\mathscr{C}^3 = \mathscr{R}_{(S_2,\pi)}(\mathscr{C}^2)$, $\mathscr{C}^4 = \mathscr{R}_{(Q_3,\pi)}(\mathscr{C}^3)$, and $\mathscr{C}^5 = \mathscr{R}_{(S_3,\pi)}(\mathscr{C}^4)$.

Under these conditions the set $\bigcup_{i=0}^{5} \mathscr{C}^i$ define the spherical tiling $\mathfrak{H}_{(\mathscr{C},\tau)}$.

Thus, for each $\tau \in \left]0, \arcsin\left(\frac{\sqrt{6}}{3}\right) + \frac{\pi}{2}\right[\setminus \{\arctan\left(\frac{\sqrt{2}}{2}\right)\}$,
the procedure described above, defines a spherical monohedral tiling with: fourteen vertices; eighteen edges; and the faces are six congruent non-convex spherical hexagons, see fig. 3.

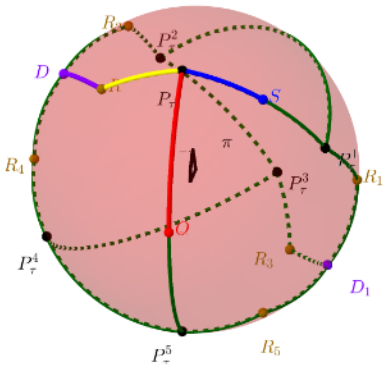

$$\begin{aligned}
D &= (\tfrac{\sqrt{3}}{3}, -\tfrac{\sqrt{3}}{3}, \tfrac{\sqrt{3}}{3}) \\
D_1 &= (-\tfrac{\sqrt{3}}{3}, \tfrac{\sqrt{3}}{3}, -\tfrac{\sqrt{3}}{3}) \\
R &= (cos(\tfrac{\pi}{4}), 0, sin(\tfrac{\pi}{4})) \\
R_1 &= (-cos(\tfrac{\pi}{4}), sin(\tfrac{\pi}{4}), 0) \\
R_2 &= (0, -cos(\tfrac{\pi}{4}), sin(\tfrac{\pi}{4})) \\
R_3 &= (-cos(\tfrac{\pi}{4}), 0, -sin(\tfrac{\pi}{4})) \\
R_4 &= (cos(\tfrac{\pi}{4}), -sin(\tfrac{\pi}{4}), 0) \\
R_5 &= (0, cos(\tfrac{\pi}{4}), -sin(\tfrac{\pi}{4})) \\
P_\tau &= (\cos(\tfrac{\pi}{4})\cos(\tau), \sin(\tfrac{\pi}{4})\cos(\tau), \sin(\tau)) \\
P_\tau^1 &= (-\cos(\tfrac{\pi}{4})\cos(\tau), \sin(\tau), \sin(\tfrac{\pi}{4})\cos(\tau)) \\
P_\tau^2 &= (-\cos(\tfrac{\pi}{4})\cos(\tau), -\sin(\tau), \sin(\tfrac{\pi}{4})\cos(\tau)) \\
P_\tau^3 &= (-sin(\tau), -cos(\tfrac{\pi}{4})cos(\tau), -sin(\tfrac{\pi}{4})cos(\tau)) \\
P_\tau^4 &= (sin(\tau), -cos(\tfrac{\pi}{4})cos(\tau), -sin(\tfrac{\pi}{4})cos(\tau)) \\
P_\tau^5 &= (\cos(\tfrac{\pi}{4})\cos(\tau), \sin(\tfrac{\pi}{4})\cos(\tau), \sin(\tau))
\end{aligned}$$

Figure 3: The tiling $\mathfrak{H}_{(\mathscr{C},\frac{\pi}{3})}$ and vertices coordinates of $\mathfrak{H}_{(\mathscr{C},\tau)}$.

When $\tau = 0$, $\mathfrak{H}_{(\mathscr{C},0)}$ is a spherical tiling by six spherical non-convex pentagons (the arc $\widehat{PQ}$ "disappeared"). We define a new cell $\mathscr{SC}$ in order to obtain the family $\mathfrak{P}_{(\mathscr{SC},\theta_1,\theta 2)}$, the detail are given next. We would like to pointed out that all tiles of these tilings have one angle of measure $\frac{2\pi}{3}$, angle that is defined by to edges, congruent to $\widehat{DR}$. In these conditions we search families of tilings by six non-convex spherical pentagons: with eleven vertices, six of them with valence two, two other vertices with valence three, and three vertices with valence four; each element of the tile has $(a,b,2b,b,a)$ edge cyclic configurations.

Using GeoGebra, with a procedure described in listing 1, we easy find the family $\mathfrak{P}_{(\mathscr{SC},\theta_1,\theta_2)}$ where $\mathfrak{H}_{(\mathscr{C},0)}$ is equal to $\mathfrak{P}_{(\mathscr{SC},\frac{\pi}{2}-\arccos\left(\frac{\sqrt{6}}{3}\right),\frac{\pi}{4})}$.

```
s:=x^2+y^2+z^2=1
t1=Slider(0, pi/2, pi/100, 1, 50, false, false, false, false)
t2=Slider(0, pi/2, pi/100, 1, 50, false, false, false, false)
V1=(0,0,1)
V2=(cos(t1),0,sin(t1))
V3=(cos(t2),sin(t2),0)
P4=(cos(t2+pi/4),sin(t2+pi/4),0)
a12=CircularArc(Centre(s),V1,V2,Plane((0,0,0),V1,V2))
a23=CircularArc(Centre(s),V2,V3,Plane((0,0,0),V2,V3))
a34=CircularArc(Centre(s),V3,V4,Plane((0,0,0),V3,P4))
SC10={a12,a23,a34}
SC11=Rotate(SC10,pi,Ray(Centre(s),V3))
SC12=Rotate({SC10,C11},2pi/3,Ray(Centre(s),V1))
SC13=Rotate(SC12,2pi/3,Ray(Centre(s),V1))
```

Listing 1: GeoGebra commands to obtain $\mathfrak{P}_{(\mathscr{SC},\theta_1,\theta_2)}$.

Now, Considering the vertices V^1, $V^2_{\theta_1}$ and $V^3_{\theta_2}$ and
$P=(\cos(\theta_2+\frac{\pi}{4}),\sin(\theta_2+\frac{\pi}{4}),0)$, see fig. 4, our new cell is the set:
$\mathscr{SC}=\{X\in S^2 : X\in \widehat{V_1V^2_{\theta_1}} \vee X\in \widehat{V^2_{\theta_1}V^3_{\theta_2}} \vee X\in \widehat{V^3_{\theta_2}P_4}\}$.

In the procedure described in listing 1, the set of spherical isometries to be considered for the local action is
$\mathscr{I}_1=\{\mathscr{R}_{(V^3_{\theta_2},\pi)},\mathscr{R}_{(V_1,\frac{2\pi}{3})}\}$
composed by two rotations. The matricial representation of the elements of $\mathscr{I}_1$ are given by:

$$\mathscr{R}_{(V^3_{\theta_2},\pi)}=\begin{pmatrix} 2\cos^2(\theta_2)-1 & 2\cos(\theta_2)\sin(\theta_2) & 0\\ 2\cos(\theta_2)\sin(\theta_2) & 2\sin^2(\theta_2)-1 & 0\\ 0 & 0 & -1\end{pmatrix};\quad \mathscr{R}_{(V_1,\frac{2\pi}{3})}=\begin{pmatrix} -\frac{1}{2} & -\frac{1}{2}\sqrt{3} & 0\\ \frac{1}{2}\sqrt{3} & -\frac{1}{2} & 0\\ 0 & 0 & 1\end{pmatrix};$$

So, let $\mathscr{SC}^0=\mathscr{SC}$ (see figure 4), $\mathscr{SC}^1=\mathscr{R}_{(V^3_{\theta_2},\pi)}(\mathscr{C}^0)$, $\mathscr{SC}^2=\mathscr{R}_{(V_1,\frac{2\pi}{3})}(\mathscr{SC}^0\cup\mathscr{SC}^1)$, $\mathscr{SC}^3=\mathscr{R}_{(V_1,\frac{2\pi}{3})}(\mathscr{SC}^2)$.

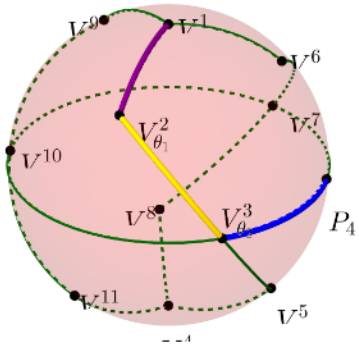

$V^1=(0,0,1)$
$V^2_{\theta_1}=(\cos(\theta_1),0,\sin(\theta_1))$
$V^3_{\theta_2}=(\cos(\theta_2),\sin(\theta_2),0)$
$V^4=(0,0,-1)$
$V^5=(\cos(2\theta_2)\cos(\theta_1),\cos(\theta_1)\sin(2\theta_2),-\sin(\theta_1))$
$V^6=\left(\frac{-\cos(\theta_1)}{2},\frac{\sqrt{3}\cos(\theta_1)}{2},\sin(\theta_1)\right)$
$V^7=\left(\frac{-\cos(\theta_2)}{2}-\frac{\sqrt{3}\sin(\theta_2)}{2},\frac{\sqrt{3}\cos(\theta_2)}{2}-\frac{\sin(\theta_2)}{2},0\right)$
$V^8=\left(-\cos(\theta_1)\sin\left(2\theta_2+\frac{\pi}{6}\right),\cos(\theta_1)\cos\left(2\theta_2+\frac{\pi}{6}\right),-\sin(\theta_1)\right)$
$V^9=\left(\frac{-\cos(\theta_1)}{2},-\frac{\sqrt{3}\cos(\theta_1)}{2},\sin(\theta_1)\right)$
$V^{10}=\left(-\frac{1}{2}\cos(\theta_2)+\frac{\sqrt{3}}{2}\sin(\theta_2),-\frac{\sqrt{3}}{2}\cos(\theta_2)-\frac{1}{2}\sin(\theta_2),0\right)$
$V^{11}=\left(\cos(\theta_1)\sin\left(2\theta_2-\frac{\pi}{6}\right),-\cos(\theta_1)\cos\left(\frac{\pi}{6}-2\theta_2\right),-\sin(\theta_1)\right)$

Figure 4: The tiling $\mathfrak{P}_{(\mathscr{SC},\frac{\pi}{4},\frac{\pi}{4})}$ and vertices coordinates of $\mathfrak{P}_{(\mathscr{SC},\theta_1,\theta_2)}$.

Under these conditions the set $\bigcup_{i=0}^{3}\mathscr{SC}^i$ defines the family of monohedral spherical tiling by non-convex spherical pentagons $\mathfrak{P}_{(\mathscr{SC},\theta_1,\theta_2)}$.

5 Conclusion

In this work, we present two new classes of monohedral tilings of the sphere $\mathfrak{H}_{(\mathscr{C},\tau)}$ and $\mathfrak{P}_{(\mathscr{SC},\theta_1,\theta_2)}$, by spherical hexagons and by spherical pentagons, respectively, extending our knowledge in this topic. It should be noted that the degenerated case $\mathfrak{H}_{(\mathscr{C},0)}$ put in evidence a monohedral tiling of the sphere by six spherical pentagons, which is part of another two parameters family of spherical tiles by non-convex spherical pentagons, that had not yet been studied. This fact reinforces the interest of GeoGebra in the study of spherical tilings.

The use of special tools created in GeoGebra, for the study of spherical tilings, have proven to be very useful in the search of new results. An important advantage of the applications created for this research is their interactivity capabilities and visualisation, promoting conjectures which where starting points for the search of formal proofs. The conjectures were also tested using the GeoGebra CAS capabilities. In future works we intend to generalise the strategy here described and apply it to other type of *cells* immersed in other spherical triangles.

6 Acknowledgments

This research was supported by the Portuguese national funding agency for science, research and technology (FCT), within the Center for Research and Development in Mathematics and Applications (CIDMA), project UID/MAT/04106/2019.

References

[1] Carlos Beltrán. A facility location formulation for stable polynomials and elliptic fekete points. *Foundations of Computational Mathematics*, 15(1):125–157, 2015.

[2] Johann S Brauchart and Peter J Grabner. Distributing many points on spheres: minimal energy and designs. *Journal of Complexity*, 31(3):293–326, 2015.

[3] Ana MR Azevedo Breda. A class of tilings of s^2. *Geometriae Dedicata*, 44(3):241–253, 1992.

[4] Ana M d'Azevedo Breda and José M Dos Santos Dos Santos. Spherical geometry and spherical tilings with geogebra. *Journal for Geometry and Graphics*, 22(2):283–299, 2018.

[5] Ana M d'Azevedo Breda and José M Dos Santos Dos Santos. Spherical tiling with geogebra - new results, challenges and open problems. *Resonance-journal of science education*, 2019in press.

[6] Ana M d'Azevedo Breda and José M Dos Santos Dos Santos. A new class of monohedral pentagonal spherical tilings with geogebra. *Portugaliae Mathematica*, 74(3):257–266, 2018.

[7] Bart De Nijs, Simone Dussi, Frank Smallenburg, Johannes D Meeldijk, Dirk J Groenendijk, Laura Filion, Arnout Imhof, Alfons Van Blaaderen, and Marjolein Dijkstra. Entropy-driven formation of large icosahedral colloidal clusters by spherical confinement. *Nature materials*, 14(1):56, 2015.

[8] Sander Dedoncker, Laurens Coox, Florian Maurin, Francesco Greco, and Wim Desmet. Bézier tilings of the sphere and their applications in benchmarking multipatch isogeometric methods. *Computer Methods in Applied Mechanics and Engineering*, 332:255 – 279, 2018.

[9] Michel Deza, Patrick W Fowler, A Rassat, and Kevin M Rogers. Fullerenes as tilings of surfaces. *Journal of chemical information and computer sciences*, 40(3):550–558, 2000.

[10] Mircea V Diudea and Csaba L Nagy. *Periodic nanostructures*, volume 7. Springer Science & Business Media, 2007.

[11] Honghao Gao, Nan Shi, and Min Yan. Spherical tiling by 12 congruent pentagons. *Journal of Combinatorial Theory, Series A*, 120(4):744 – 776, 2013.

[12] Giuliana Indelicato, Newton Wahome, Philippe Ringler, Shirley A Müller, Mu-Ping Nieh, Peter Burkhard, and Reidun Twarock. Principles governing the self-assembly of coiled-coil protein nanoparticles. *Biophysical journal*, 110(3):646–660, 2016.

[13] Walter Kohn. An essay on condensed matter physics in the twentieth century. *Reviews of Modern Physics*, 71(2):S59, 1999.

[14] Joachim König, Arielle Leitner, and Danny Neftin. Almost-regular dessins d'enfant on a torus and sphere. *Topology and its Applications*, 243:78 – 99, 2018.

[15] Majid Mosayebi, Deborah K Shoemark, Jordan M Fletcher, Richard B Sessions, Noah Linden, Derek N Woolfson, and Tanniemola B Liverpool. Beyond icosahedral symmetry in packings of proteins in spherical shells. *Proceedings of the National Academy of Sciences*, 114(34):9014–9019, 2017.

[16] Manica Negahdaripour, Nasim Golkar, Nasim Hajighahramani, Sedigheh Kianpour, Navid Nezafat, and Younes Ghasemi. Harnessing self-assembled peptide nanoparticles in epitope vaccine design. *Biotechnology advances*, 35(5):575–596, 2017.

[17] Ali Asghar Rezaei. Polygonal tiling of some surfaces containing fullerene molecules. *Iranian Journal of Mathematical Chemistry*, 5(2):99–105, 2014.

[18] Ali Asghar Rezaei. Tiling fullerene surface with heptagon and octagon. *Fullerenes, Nanotubes and Carbon Nanostructures*, 23(12):1033–1036, 2015.

[19] Yuan-Zhi Tan, Rui-Ting Chen, Zhao-Jiang Liao, Jia Li, Feng Zhu, Xin Lu, Su-Yuan Xie, Jun Li, Rong-Bin Huang, and Lan-Sun Zheng. Carbon arc production of heptagon-containing fullerene [68]. *Nature communications*, 2:ncomms1431, 2011.

[20] Yukako Ueno and Yoshio Agaoka. Tilings of the 2-dimensional sphere by congruent right triangles. *Memoirs of the Faculty of Integrated Arts and Sciences, Hiroshima University. IV, Science reports: studies of fundamental and environmental sciences*, 22:1–23, 1996.

[21] Yukako Ueno, Yoshio Agaoka, et al. Classification of tilings of the 2-dimensional sphere by congruent triangles. *Hiroshima Mathematical Journal*, 32(3):463–540, 2002.

[22] Zhi Wang, Hai-Feng Su, Yuan-Zhi Tan, Stan Schein, Shui-Chao Lin, Wei Liu, Shu-Ao Wang, Wen-Guang Wang, Chen-Ho Tung, Di Sun, et al. Assembly of silver trigons into a buckyball-like ag180 nanocage. *Proceedings of the National Academy of Sciences*, 114(46):12132–12137, 2017.